Geomechanics and Engineering, *Vol. 27, No. 5 (2021) 447-463*
https://doi.org/10.12989/gae.2021.27.5.447

Seismic behavior of caisson-type gravity quay wall renovated by rubble mound grouting and deepening

Young-Sang Kim*[1], Anh-Dan Nguyen[2a] and Gyeong-O Kang[3b]

[1]*Department of Civil Engineering, Chonnam National University, Gwangju, South Korea*
[2]*Department of Architecture and Civil Engineering, Graduate school, Chonnam National University, Gwangju, South Korea*
[3]*Department of Civil Engineering, Gwangju University, Gwangju, South Korea*

(Received June 12, 2021, Revised August 16, 2021, Accepted October 8, 2021)

Abstract. Caisson-type structures are widely used as quay walls in coastal areas. In Korea, for a long time, many caisson-type quay walls have been constructed with a low front water depth. These facilities can no longer meet the requirements of current development. This study developed a new technology for deepening existing caisson-type quay walls using grouting and rubble mound excavation to economically reuse them. With this technology, quay walls could be renovated by injecting grout into the rubble mound beneath the front toe of the caisson to secure its structure. Subsequently, a portion of the rubble mound was excavated to increase the front water depth. This paper reports the results of an investigation of the seismic behavior of a renovated quay wall in comparison to that of an existing quay wall using centrifuge tests and numerical simulations. Two centrifuge model tests at a scale of 1/120 were conducted on the quay walls before and after renovation. During the experiments, the displacements, accelerations, and earth pressures were measured under five consecutive earthquake input motions with increasing magnitudes. In addition, systematic numerical analyses of the centrifuge model tests were also conducted with the PLAXIS 2D finite element (FE) program using a nonlinear elastoplastic constitutive model. The displacements of the caisson, response accelerations, deformed shape of the quay wall, and earth pressures were investigated in detail based on a comparison of the numerical and experimental results. The results demonstrated that the motion of the caisson changed after renovation, and its displacement decreased significantly. The comparison between the FE models and centrifuge test results showed good agreement. This indicated that renovation was technically feasible, and it could be considered to study further by testbed before applying in practice.

Keywords: caisson-type gravity quay wall; centrifuge model test; deepening; numerical simulation; renovated quay wall

1. Introduction

Currently, there is a demand for deep-water ports with high earthquake resistance because of the increase in transportation via waterways by large tonnage ships and the challenges of withstanding natural disasters. However, many of the quay walls constructed in the past cannot meet the requirements of current development. In addition, replacing the existing structures with new quay walls is not the preferred solution because of the high cost and environmental problems. Thus, renovating existing quay walls to enhance their performance and ensure earthquake resistance is a significant challenge for researchers and engineers.

Several previous case studies have been conducted on the renovation of quay walls. Bauduin *et al*. (2017) suggested some general guidelines for quay wall renovation to obtain an integrated design and construction approach that included construction methods, risk management, and monitoring. The study provided some elements of guidance for the different aspects based on experience gained in real projects of several kinds and indicates tools to deal with insufficient or less reliable information by use of fault tree, robust design, and flexible execution methods combined with monitoring and observational methods. Oung and Brassinga (2015) studied the redesign of an existing quay wall from the perspective of risk assessment. The research focused on describing the initial conditions and situations, the risks that could occur during rebuilding, the risk mitigation measures, and some uncertainties that still existed. They concluded that the lack of information in the current situation constitutes the main obstacle to a straightforward redesign and the use of finite element method modeling reveals a failure mechanism, which was not encountered earlier. Because of the technical risks, a redesign of such existing and complex quay wall would necessitate an extensive design procedure to increase reliability. Ruggeri *et al*. (2019) summarized the main problems related to geotechnical engineering during the design and construction of upgraded quay walls in Italy. To enhance the performance of six quay walls, several methods were considered, which focused on the use of micro-piles and jet grouting to increase the bearing capacity and front water depth. Galal (2017) proposed the use of new box

*Corresponding author, Professor
E-mail: geoyskim@jnu.ac.kr
[a] Ph.D. Candidate
E-mail: nadan.jnu@gmail.com
[b] Professor
E-mail: gokang@gwangju.ac.kr

ISSN: 2005-307X (Print), 2092-6219 (Online)

sheet pile panels installed in front of the wall and then excavating the soil to increase the front water depth of the existing open berth quay wall in Egypt. The authors conducted finite element (FE) analyses to assess and compare the behaviors in the pre-upgrading and post-upgrading cases. The structure was strengthened by an additional structure system that included piles and sheet piles before excavating the seabed. Nguyen *et al*. (2021) studied the static behavior after deepening the front water depth of a caisson-type quay wall by excavating a portion of the rubble mound after grouting. The research considered various cases to determine the most suitable shape and dimensions of the grouted rubble. Based on analysis of the stability of specific quay wall case, construction method, and economic perfective, the paper found that the most suitable size of grouted rubble was 3 m x 3 m with an oblique cutting plane in front of the wall.

Some researchers have conducted both experimental and numerical analyses of the dynamic behavior of quay walls. Inagaki *et al*. (1996) assessed the seismic performance of caisson-type quay walls in Kobe based on an in-situ investigation after the 1995 Hyogoken Nambu earthquake. The results focused on the access displacements of the caisson and rubble mound. In addition, a shaking table test was conducted to compare the investigated results and consider the excess pore pressure change in the backfill. Based on the contrast between the damaged and undamaged quay walls as well as in-situ geotechnical investigations and shake table tests, the paper presented essential data and discussed to understand how serious damage occurred to many of the caisson type quay walls. Alyami *et al*. (2009), Dakoulas and Gazetas (2008), Galavi *et al*. (2013) also used numerical analyses with distinct soil models to analyze the dynamic response of the caisson and excess pore pressure development in the backfill of the quay walls in the Kobe port. Lee (2005) performed several centrifuge tests to model the behavior of the gravity quay wall in Taichung port using the input motion and data from an investigation of the 1999 Chichi earthquake. The test results showed that the rotational mode made the dominant contribution to the changes in excess pore water pressure and the earth pressure in the deep layers of soil, but the translational mode made the dominant contribution to these pressures in the shallow layers. The average shear wave velocities were found to decrease rapidly to values as low as 1/8th of the velocity measured at the beginning of shaking. Mizutani and Kikuchi (2013) conducted shaking table tests on caisson-type quay walls with the stabilized mound. The tests evaluated the variation of vibrational properties and deformation mode caused by the different shapes of the solidified area. By comparison to the existing case, the authors indicated that the attendance of stabilized mound block changed deformation mode and decreased displacement of the caisson. Cihan *et al*. (2015) considered the responses of block-type gravity quay walls under dynamic loading by comparing numerical modeling and shaking table test results. The acceleration, soil pressure, pore pressure, and displacement were measured and analyzed. In addition, a numerical study was conducted using PLAXIS V8.2. Dakoulas *et al*. (2018) used four numerical models to assess the movement of blocks, foundations, and backfill during an earthquake. The study demonstrated that, for constant average relative density, the effects of its spatial variability were smaller than the effects of the frequency characteristics of the earthquake excitation. Moreover, a foundation of high relative density might significantly decrease settlements and rotation of the wall, but some reduced horizontal displacements caused partly by block-to-block sliding may still take place. Excess pore-water pressures immediately behind the wall were mostly negative, increasing the soil resistance.

Based on the above literature, although there have been some studies related to the renovation and dynamic behavior assessment of existing quay walls, there is still a need for studies on the seismic responses of renovated quay walls. Therefore, this study evaluated and compared the seismic behavior of a renovated caisson-type gravity quay wall with that of the existing wall using a centrifuge model test and numerical simulation. The cross-sections of the quay wall examined in this study before and after renovation are shown in Fig. 1. The wall was designed based on an example provided by the Ministry of Ocean and Fisheries-Korea (2018). The goal of the renovation was to increase the front water depth from 13.5 m to 15.5 m by deepening the rubble in front of the caisson. To ensure the stability of the quay wall, the rubble mound beneath the caisson front toe was solidified by grouting before excavation. The shape and dimensions of the grouted rubble were determined by checking its stability, strength, and construction feasibility based on the study by Nguyen *et al*. (2021). Centrifuge model tests were performed for both the existing quay wall and the renovated quay wall. In addition, numerical simulations of the centrifuge models were performed to determine reasonable material properties and suggest an accurate numerical method to use for the analysis. This study analyzed the dynamic response of the

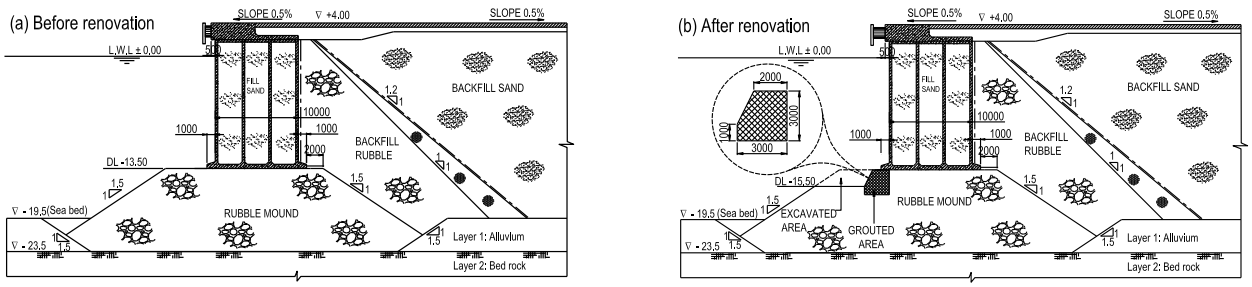

Fig. 1 Cross sections of quay walls examined in this study

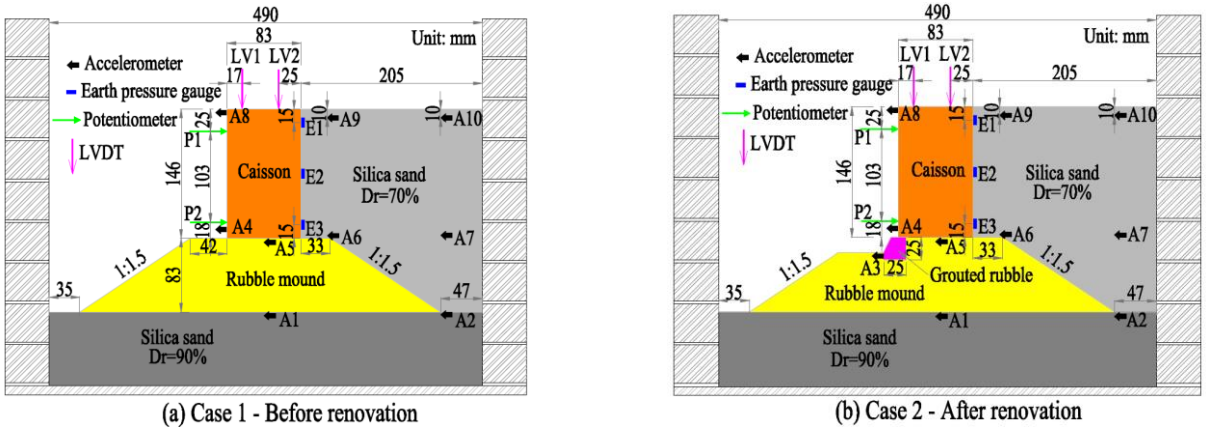

Fig. 2 Model layout

Table 1 Scaling factors of various variables in centrifuge model test (Iai *et al*. 2005)

Quantity	Partitioned				Scaling factor (prototype/physical model)	
	Virtual 1 g field		Centrifugal field		Equation	Value
Length	μ	3	η	40	$\mu\eta$	120
Density	μ_ρ	1	*1*	1	μ_ρ	1
Time	$(\mu\mu_\varepsilon)^{0.5}$	2.280	η	40	$(\mu\mu_\varepsilon)^{0.5}\eta$	91.180
Frequency	$(\mu\mu_\varepsilon)^{-0.5}$	0.439	$1/\eta$	0.025	$(\mu\mu_\varepsilon)^{-0.5}/\eta$	0.011
Acceleration	*1*	1	$1/\eta$	0.025	$1/\eta$	0.025
Velocity	$(\mu\mu_\varepsilon)^{0.5}$	2.280	*1*	1	$(\mu\mu_\varepsilon)^{0.5}$	2.280
Displacement	$\mu\mu_\varepsilon$	5.296	η	40	$\mu\mu_\varepsilon\eta$	207.846
Stress	$\mu\mu_\rho$	3	*1*	1	$\mu\mu_\rho$	3
Strain	$\mu_\varepsilon=\mu^{0.5}$	1.732	*1*	1	μ_ε	1.732

quay wall in detail, including the caisson displacement, deformed shape of the quay wall, settlement of the backfill, and earth pressure.

2. Dynamic centrifuge testing program

2.1 Centrifuge apparatus and scaling factors

The experiments were conducted at the KAIST Geotechnical Centrifuge Testing Center (Korea). The maximum capacity of the centrifuge apparatus was 240 g-tons with a platform radius of 5 m. An earthquake simulator was installed on the centrifuge, together with an electro-hydraulic device used to simulate seismic loading during flight. This system can create random seismic excitations with a duration of up to 2 s and a frequency range of 40–300 Hz. The base shaking acceleration of the equipment can reach 20 g under a maximum payload of 700 kg, which corresponds to 0.5 g of horizontal acceleration on a prototype scale at 40 g of centrifugal acceleration (Cho *et al*. 2018, Kim *et al*. 2013, Ngo *et al*. 2019).

To reduce the effect of the boundary conditions on the behavior of the soil and structure, an equivalent shear beam (ESB) container was used in the tests. The ESB model container at KAIST was formed by stacking 10 lightweight aluminum rectangular alloy frames on the base plate to create internal dimensions of 490 × 490 × 630 mm and external dimensions of 650 × 650 × 650 mm. The height of each frame was 60 mm, and they were separated by ball bearings and rubble spacing layers. The design concept was that the deflection of each frame and soil near the frame was the same. Thus, it had dynamic stiffness and natural frequency similar to that of the inside model (Ha *et al*. 2014, Zeng and Schofield 1996, Cho *et al*. 2020).

Two dynamic centrifuge tests were performed for the caisson-type gravity quay wall before and after renovation. The centrifuge models were designed based on the cross-sections shown in Fig. 1. The tests used the concept of the two-stage scale suggested by Iai *et al*. (2005), with a scaling factor of 120 g. The scaling factors are listed in Table 1.

2.2 Model preparation

Figs. 2(a) and 2(b) present the cross-sections of the testing models with the sensor arrangement for quay walls before renovation (case 1) and after renovation (case 2), respectively. For each model, the horizontal displacements of the caisson were measured using two potentiometers, while the vertical displacement was measured by two LVDT sensors installed on the top surface of the caisson. It was noticed that data received from the potentiometers or LVDT sensors could also be used to calculate the rotation of the caisson. Three earth pressure gauges were attached to the back of the caisson to measure the earth pressure. The acceleration time histories of the caisson, soil, and rubble

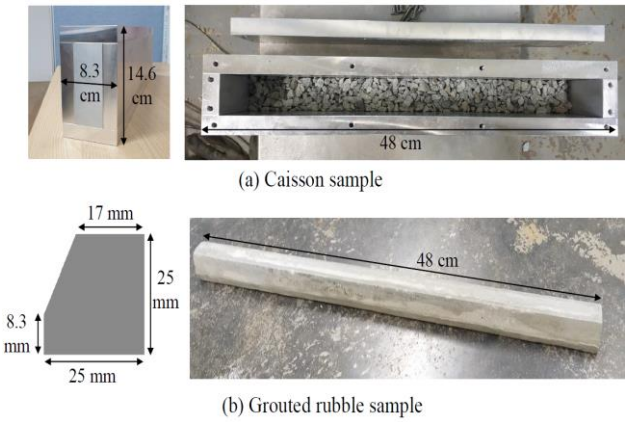

Fig. 3 Caisson and grouted rubble sample preparation

Table 2 Properties of silica sand and rubble

Silica sand		*Rubble*	
Parameters	Value	Parameters	Value
Soil classification, USCS	SP	Particle size (cm)	0.5×1
Uniformity coefficient, C_u	1.482	Maximum density, γ_{max} (kN/m^3)	15.95
Curvature coefficient, C_c	1.071	Minimum density, γ_{min} (kN/m^3)	12.51
Effective particle size, D_{10}	0.218		
Specific gravity, G_s	2.65		
Maximum density, γ_{max} (kN/m^3)	15.84		
Minimum density, γ_{min} (kN/m^3)	12.55		

were recorded using horizontal accelerometers buried at different locations in the models.

Fig. 3 shows the detailed structure and dimensions of the caisson and grouted rubble block models. The caisson model used in the experiments was made from an aluminum alloy, while the grouted rubble was made from cement paste. The weight of the caisson was determined by the weight of the aluminum and added rubble inside the caisson. The centrifuge tests were conducted under dry condition. For this simplification, problems involved the excess pore pressure could not be evaluated. However, since relative density of backfill was about 70%, consideration of the problem related to liquefaction was not necessary.

The bedrock and backfill were composed of poorly graded clean silica sandy soil (SP). The sand was prepared using a sand raining system with relative densities for the bedrock and backfill of 90% and 70%, respectively. The rubble was made and compacted by hand with a relative density of approximately 70%. The properties of the silica sand and rubble are listed in Table 2.

Fig. 4 illustrates the model construction process. The sequence included five steps. First, the ESB container was filled with the bottom sand layer to the design level using the raining system. Second, the rubble mound layer was carefully formed by dividing it into several layers stacked on top of each other with slopes and heights based on the design. In case 2, the rubble mound was created first, reaching the bottom of the grouted rubble block. Subsequently, the grouted rubble block was installed before the remainder of the rubble was filled to the surface of the rubble mound. Third, the surface of the rubble mound was flattened, and the caisson was placed at the determined location. A balance ruler was used to control the equilibrium of the caisson. Fourth, the raining system was used to introduce backfill up to the quay wall surface level. The sand leached out in front of the quay wall during construction was carefully cleaned up using a vacuum. Finally, the accelerometers, LVDT sensors, and potentiometers were set up. It should be noted that all the measuring instruments inside the sand and rubble were placed at the designed locations during the construction of the model. In addition, the balance of the caisson was ensured by the balance ruler during the entire construction.

2.3 Input earthquake motion

Centrifuge tests were conducted with five consecutive earthquake motions. The input signal was based on the Hachinohe earthquake wave, but different multiplier factors were used to create a distinct acceleration time series with increasing magnitude. In reality, because of the sensitivity of the system and sample conditions, there was a difference between the accelerations assigned to the models of the quay wall before and after renovation. However, this difference was relatively small; thus, they could be considered the same for both cases. The details of the earthquake input motions used in the centrifuge tests and numerical analyses are shown in Fig. 5. These values were presented on a prototype scale.

3. Numerical analysis

3.1 Constitutive model of soil

The behavior of the silica sand and rubble in the analysis was described using a constitutive model, namely the Hardening soil model with small-strain stiffness (HS-small). The HS-small model was developed by Benz (2007) based on the hardening soil model designed by Schanz *et al*. (1999). The HS-small model was formulated to reproduce macroscopic phenomena exhibited by soil, such as its densification, stress-dependent stiffness, soil stress history, plastic yielding, and dilatation. In particular, it can handle other observed properties of the sand in the small strain domain, including a strong stiffness variation with the development of the shear strain amplitude, and a hysteretic, nonlinear elastic stress-strain relationship. These features indicate that the HS-small model is suitable for producing a more accurate and reliable approximation of displacements, which can be useful for dynamic applications. The details of the HS-small model can be found in the literature (PLAXIS 2018, Obrzud and Truty 2018). The basic parameters of the model include the cohesion (c), friction angle (ϕ), angle of dilatancy (ψ), secant stiffness in the standard drained triaxial test (E_{50}^{ref}), tangent stiffness for the primary oedometer loading (E_{oed}^{ref}), unloading/reloading stiffness (E_{ur}^{ref}), power for the stress-level dependency of the

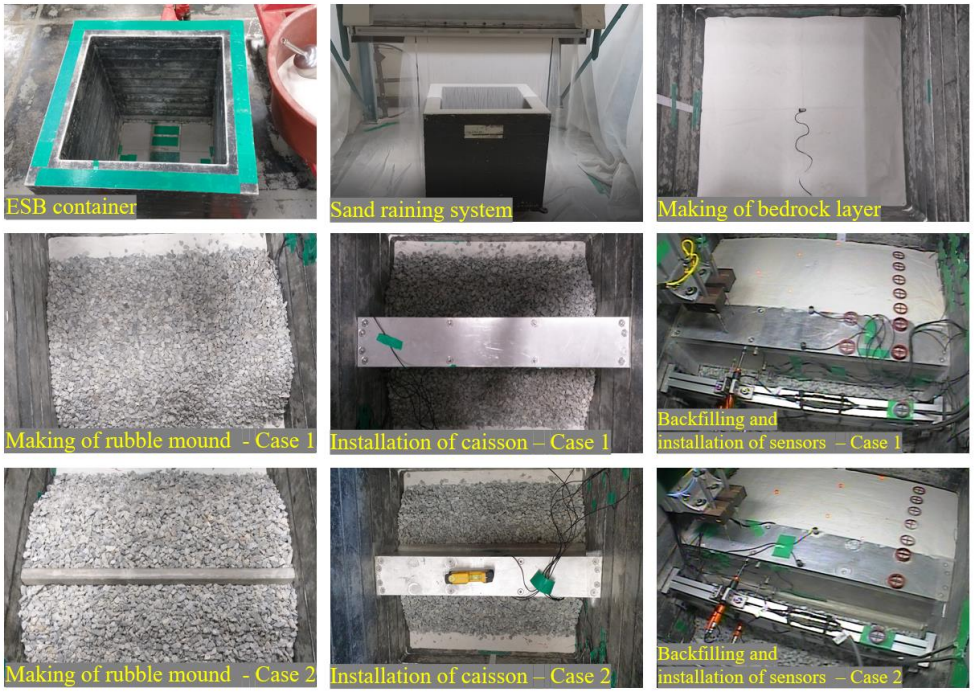

Fig. 4 Model construction process for centrifuge test

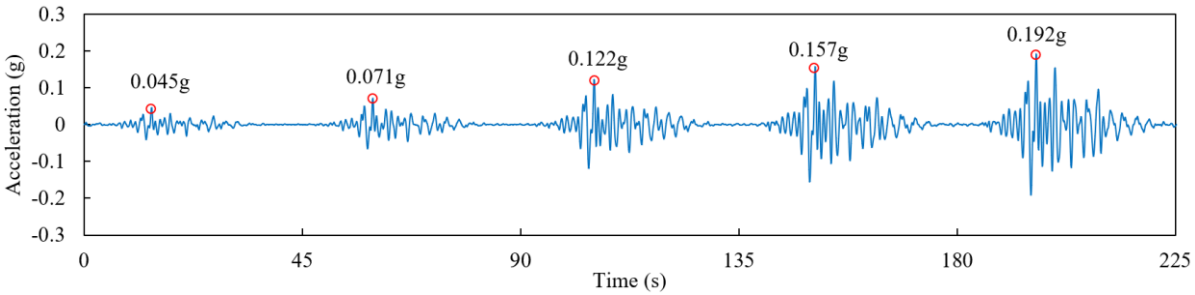

Fig. 5 Earthquake input motion used in centrifuge tests and numerical analyses (prototype scale)

stiffness (m), Poisson's ratio (v_{ur}), reference shear modulus at very small strains (G_0^{ref}), and threshold shear strain at which $G_s = 0.722G_0$ ($\gamma_{0.7}$) (PLAXIS 2018).

Table 3 lists the basic parameters of the materials used in the models, as determined by laboratory experiments. Table 4 summarizes the model parameters for the two relative densities. The stiffness characteristics of the sand and rubble were extracted first based on the relative density, D_r, of the material found using the relative equations proposed by Brinkgreve *et al*. (2010), as shown in Eqs. 1, 2, and 3. To determine the initial shear modulus, G_o, and shear strain, $\gamma_{0.7}$, some resonant column tests were conducted by KAIST for silica sand with relative densities of 90% and 70%. All the parameters were backfitted and validated in the subsequent parametric analysis.

$$E_{50}^{ref} = 60000D_r \quad \text{(kPa)} \tag{1}$$

$$E_{oed}^{ref} = 60000D_r \quad \text{(kPa)} \tag{2}$$

$$E_{ur}^{ref} = 180000D_r \quad \text{(kPa)} \tag{3}$$

Table 3 Basic parameters of materials

Layers	Relative density Dr (%)	Elastic modulus E (kPa)	Unit weight γ (kN/m^3)	Friction angle ϕ (°)
Bottom sand	90		15.45	40
Backfill	70		14.70	37
Rubble	70		14.73	40
Caisson wall		30×10^6	21.00	
Grouted rubble		20×10^6	20.00	

Table 4 Model parameters (at $p^{ref} = 100$ kPa)

Material parameters	Unit	$D_r = 90\%$	$D_r = 70\%$
E_{50}^{ref}	kPa	54,000	42,000
E_{oed}^{ref}	kPa	54,000	42,000
E_{ur}^{ref}	kPa	162,000	126,000
m	-	0.5	0.5
v_{ur}	-	0.2	0.2
G_0^{ref}	kPa	100,000	80,000
$\gamma_{0.7}$	(%)	0.06	0.06

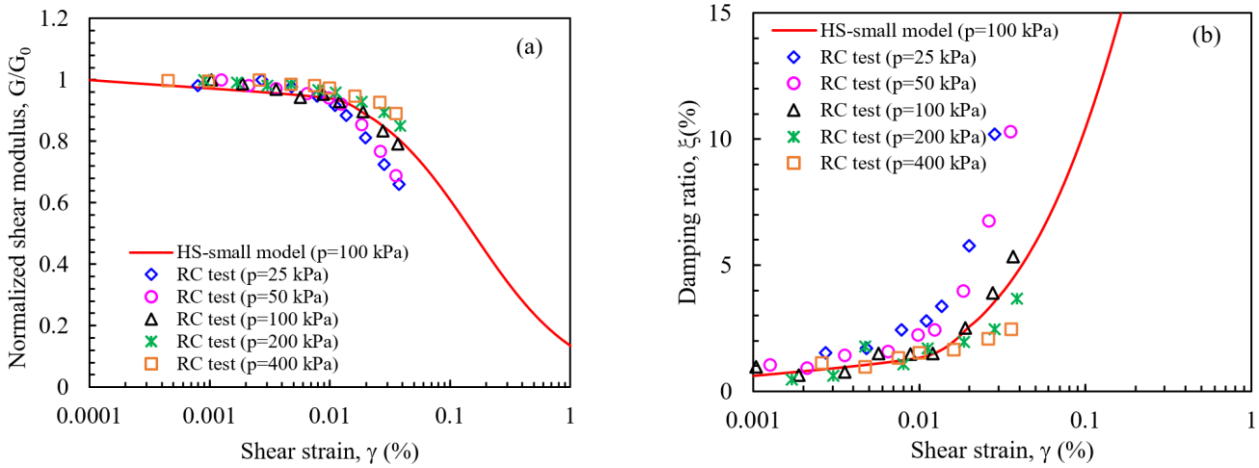

(a) Normalized shear modulus versus shear strain (b) Damping ratio versus shear strain

Fig. 6 Comparison of model prediction and resonant column test results of Silica sand (Dr = 90%)

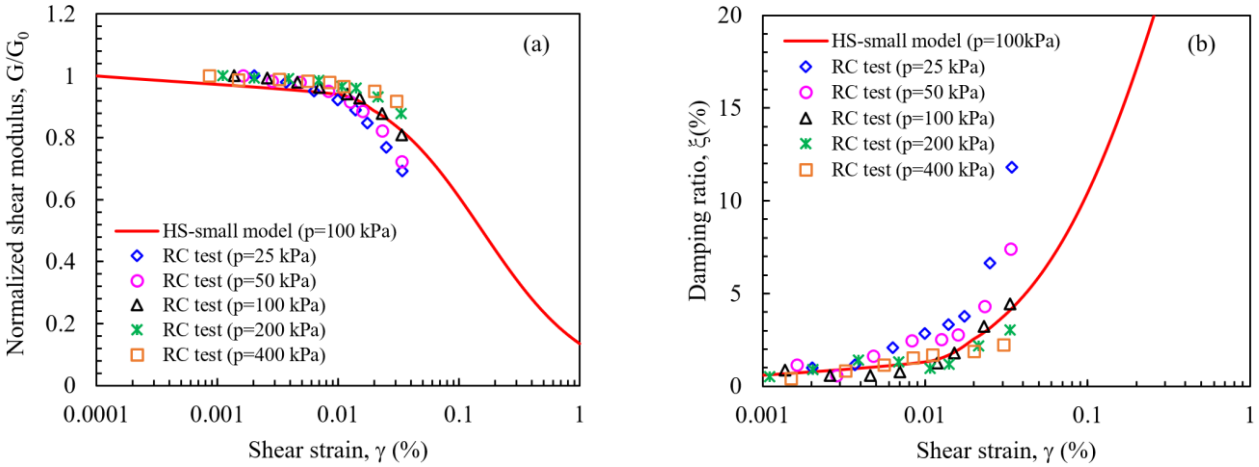

(a) Normalized shear modulus versus shear strain (b) Damping ratio versus shear strain

Fig. 7 Comparison of model prediction and resonant column test results of Silica sand (Dr = 70%)

Figs. 6 and 7 show comparisons of the results from the resonant column (RC) tests and model prediction for the relative densities of 90% and 70%, respectively. In each figure, the left graph shows the relationship between the normalized shear modulus (G/G_o) and cyclic shear strain, while the right graph shows the increase in the damping ratio (ξ) in relation to the cyclic shear strain. It can be seen that the test results were captured well with the numerical simulation. This indicated that the HS-small model could simulate the seismic behavior of models made of silica sand.

3.2 Finite element simulation

To evaluate and compare the numerical model and centrifuge test results for the behavior of the quay wall, two-dimensional FE analyses were conducted using the PLAXIS 2D CE program on a prototype scale under conditions similar to those of the centrifuge tests. In the centrifuge tests, the ESB container was used to avoid reflected waves due to the fixed boundaries. In the numerical model, the ESB container was also simulated as shear beams with aluminum alloy frames and rubber spacing layers using a linear elastic model (Gerolymos *et al*. 2015, Al-Homoud and Whitman 1995, Pitilakis *et al*. 2004). In addition, Visco dashpots were placed on both side boundaries of the models, allowing a response similar to that of the ESB container (Galavi *et al*. 2013, PLAXIS 2018). A fixed base boundary was used for the bottom boundary, and prescribed displacements were imposed to prevent movement in the vertical direction (Pitilakis *et al*. 2004, Gerolymos *et al*. 2015, Ha and Han 2016).

The interaction between the soil and the caisson was simulated by interface elements to consider the gapping and slippage via the Coulomb friction law. The interface angle was taken as 0.7 times the internal friction angle of the soil (Athanasopoulos-Zekkos *et al*. 2013). Thus, the calculated interface angles were 26° and 28° at the back and base of the caisson, respectively. Similarly, the interface elements along the contact edges between the soil and the ESB container model were assigned an interface angle of 26°.

As previously mentioned, in the tests, the relative density of the bottom sand layer was 90%, while the density of the backfill and rubble was 70%. In the analyses, these layers were simulated using the HS-small model. The caisson, grouted rubble, and ESB container were modeled

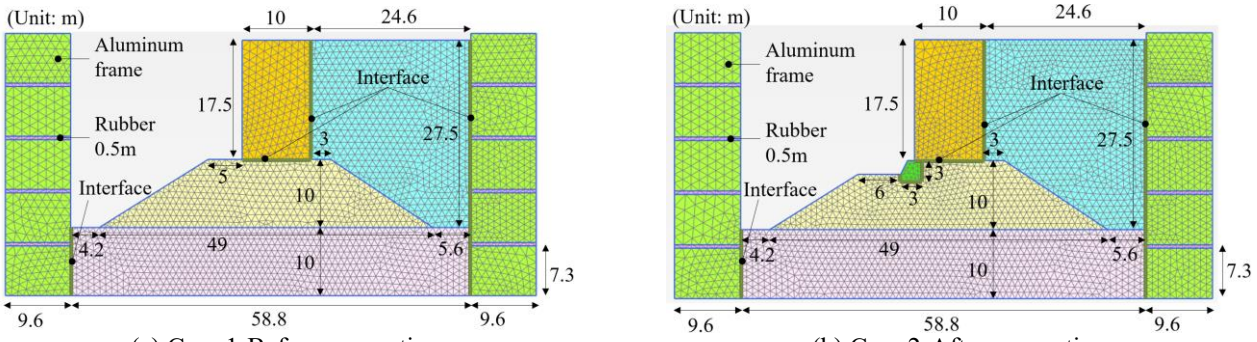

(a) Case 1-Before renovation (b) Case 2-After renovation

Fig. 8 Finite element models of centrifuge tests

using the linear elastic model. All the materials were modeled using 15 node triangular plane strain elements. The average element size, Δl, of the models was approximately 0.8 m. It was preliminarily defined based on the recommendation of Kuhlemeyer and Lysmer (1973) to guarantee a proper propagation of the shear wave in the finite element method according to Eqs. 4 and 5. After that, it was selected based on a sensitivity analysis.

$$\Delta l \le \frac{\lambda}{10} \sim \frac{\lambda}{8} \tag{4}$$

$$\lambda = \frac{V_s}{f_{\max}} \tag{5}$$

where λ is the wavelength of the maximum frequency of interest, f_{max}; V_s is shear wave velocity. Before performing the seismic analysis, static analysis was conducted to calculate the initial status of the ground due to gravity loading on the prototype scale under conditions similar to those of the centrifuge tests. After finishing the initial phase, the analysis was automatically transferred to the dynamic analysis. The earthquake input motions were the same as those used in the centrifuge test, including five consecutive waves, as shown in Fig. 5. The FE models for both cases are shown in Fig. 8.

When using the HS-small model, the amount of damping that is obtained depends on the amplitude of the strain cycles. When considering very small vibrations, the model does not exhibit material damping, whereas real soils still show some viscous damping. Hence, additional damping is required to model the realistic damping characteristics of soils in dynamic calculations. This can be achieved by Rayleigh damping (PLAXIS 2018). Damping matrix C can be interpreted from mass matrix M and stiffness matrix K by Eq. 6.

$$C = \alpha M + \beta K \tag{6}$$

where α and β are Rayleigh coefficients, which are estimated based on the relationship between the damping ratio, ξ, and target frequencies, ω_1 and ω_2, according to Eq. 7.

$$\alpha = \frac{2\omega_1\omega_2}{\omega_1 + \omega_2}\xi; \beta = \frac{2}{\omega_1 + \omega_2}\xi \tag{7}$$

In this study, the critical damping ratio was 5% for the wall and grouted rubble and 2% for the soil and rubble (Arablouei *et al*. 2011). The target frequencies were determined as $\omega_1 = 2\pi f_1$ and $\omega_2 = 2\pi f_4$, in which f_1 and f_4 were frequencies of first and fourth modes estimated from free vibration analysis of the models (Chopra 2001). Based on analyses, the frequencies of case 1 were $f_1 = 1.24$ and $f_4 = 4.06$ Hz. The calculated damping parameters, α and β, for the caisson were 0.59683 and 3.0029×10^{-3}, respectively; while the values for the sand and rubble were 0.23873 and 1.2011×10^{-3}, respectively. Similarly, the target frequencies of case 2 were $f_1 = 1.28$ and $f_4 = 4.14$ Hz. The values of α and β were 0.61431 and 2.9364×10^{-3} for the caisson and grouted rubble, respectively; and 0.24572 and 1.1746×10^{-3} for the soil and rubble, respectively.

4. Results and discussion

4.1 Displacement and tilting of caisson

Figs. 9 and 10 show the horizontal and vertical displacements at the top left corner (point A) of the caisson in case 1 (before renovation) and case 2 (after renovation), respectively. The horizontal displacements at point A were obtained based on the analysis results measured using two potentiometers P1, P2, and accelerometer A8. The vertical displacement was calculated using two LVDT sensors. In each figure, the upper half of the graph compares the centrifuge model test and numerical analysis displacements of case 1, while the case 2 comparison is plotted in the lower half. Positive movements were assumed to be toward the right side and in the upward direction of the models. All results herein are presented on prototype scale.

It can be seen that in both cases, the caisson showed horizontal displacements that were larger than the vertical displacements. In addition, both the horizontal and vertical displacements of the caisson decreased significantly after renovation. The displacements increased with the magnitude of the input motion. From the test results in Fig. 9, before the renovation, the maximum horizontal displacements were 6.68, 15.44, and 22.98 cm at steps 1, 3, and 5, respectively. After the renovation, these values decreased to 6.04, 11.99, and 18.52 cm at the same stages. A similar tendency is observed in Fig. 10 for the vertical

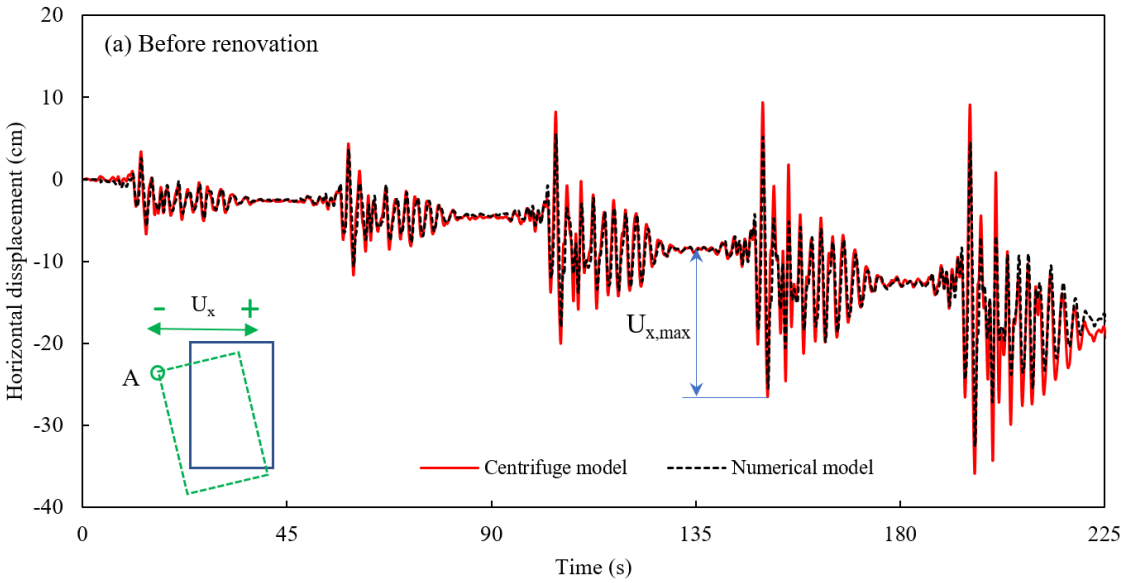

Maximum horizontal displacement ($U_{x,max}$) at each step

(Unit: cm)	Step 1	Step 2	Step 3	Step 4	Step 5
Centrifuge model	-6.68	-9.17	-15.44	-17.86	-22.98
Numerical model	-5.70	-8.16	-13.76	-16.63	-19.79

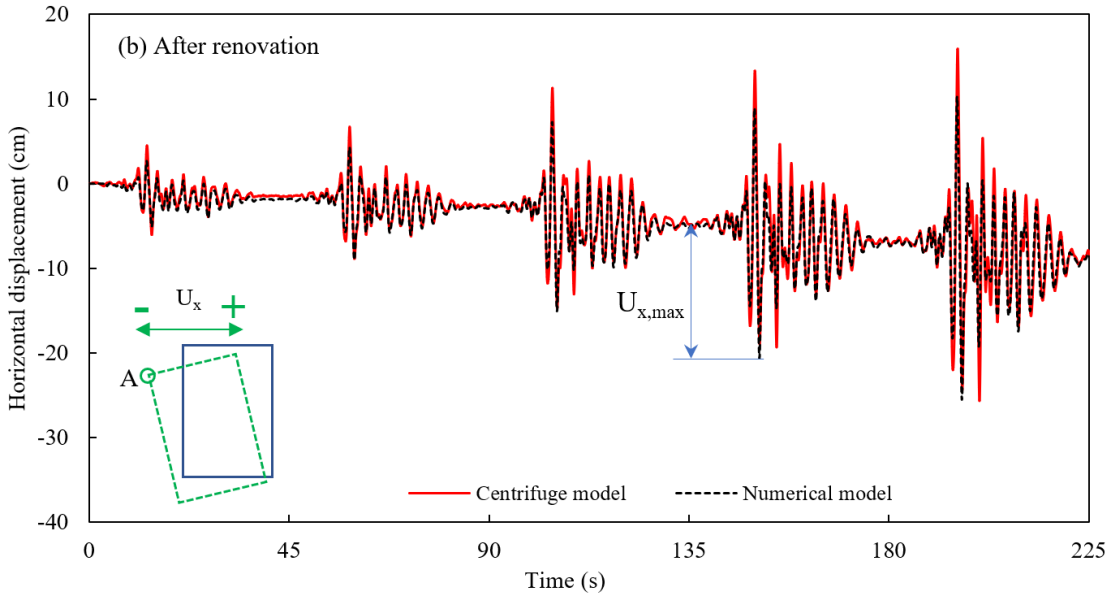

Maximum horizontal displacement ($U_{x,max}$) at each step

(Unit: cm)	Step 1	Step 2	Step 3	Step 4	Step 5
Centrifuge model	-6.04	-7.43	-11.99	-14.51	-18.52
Numerical model	-5.10	-7.21	-12.13	-15.37	-18.38

Fig. 9 Horizontal displacements at top left corner (Point A) of caisson

displacement. At step 1, the vertical displacements were almost similar for both cases, at 0.93 cm for case 1 and 0.90 cm for case 2. When the amplitude of the earthquake input motion increased, the vertical displacements of the renovated case at steps 3 and 5 were 2.10 and 3.48 cm, respectively, which were lower than those of the existing quay wall case at 3.97 and 6.49 cm, respectively.

To access the possibility of damage of the caisson–type quay wall during earthquake, the Harbor and Fishing port design standard (Ministry of Ocean and Fisheries-Korea, 2018) suggested using the ratio between horizontal displacement and height of the wall (U_x/H). The allowable ratio is U_x/H = 1.5%. If this ratio is larger than 1.5 %, significant damage will occur in the main body of the wall. From the test results, the maximum horizontal displacement of the quay wall was before the renovation was 22.98 cm, thus the ratio U_x/H = 1.33%. Although this value still satisfied the standard requirement, it was close to the

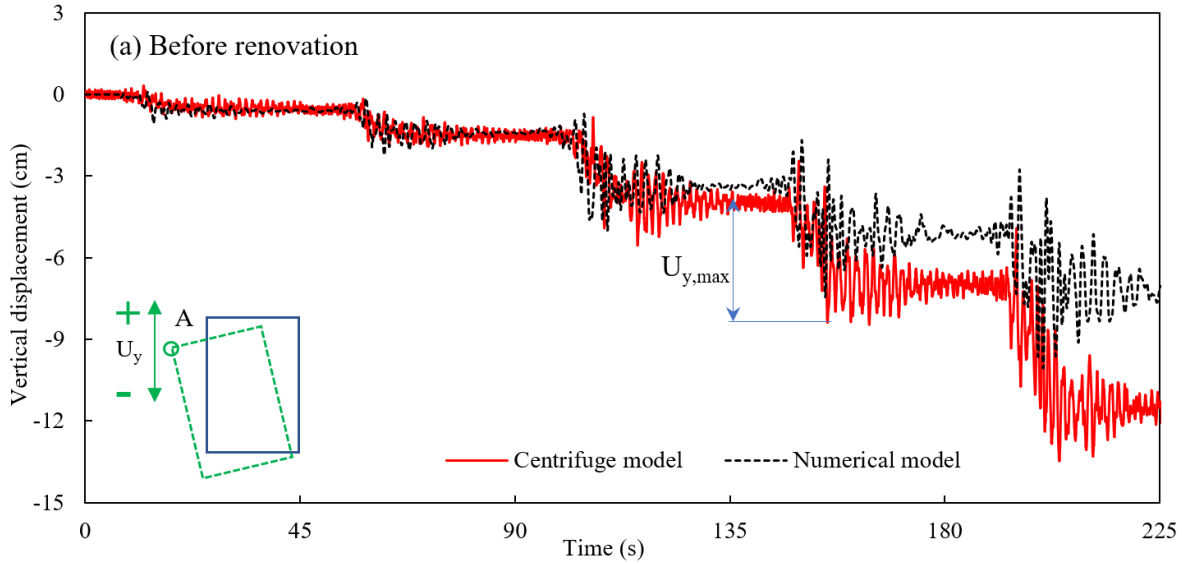

Maximum vertical displacement ($U_{y,max}$) at each step

(Unit: cm)	Step 1	Step 2	Step 3	Step 4	Step 5
Centrifuge model	-0.93	-1.64	-3.97	-4.43	-6.49
Numerical model	-1.07	-1.64	-3.57	-3.94	-5.18

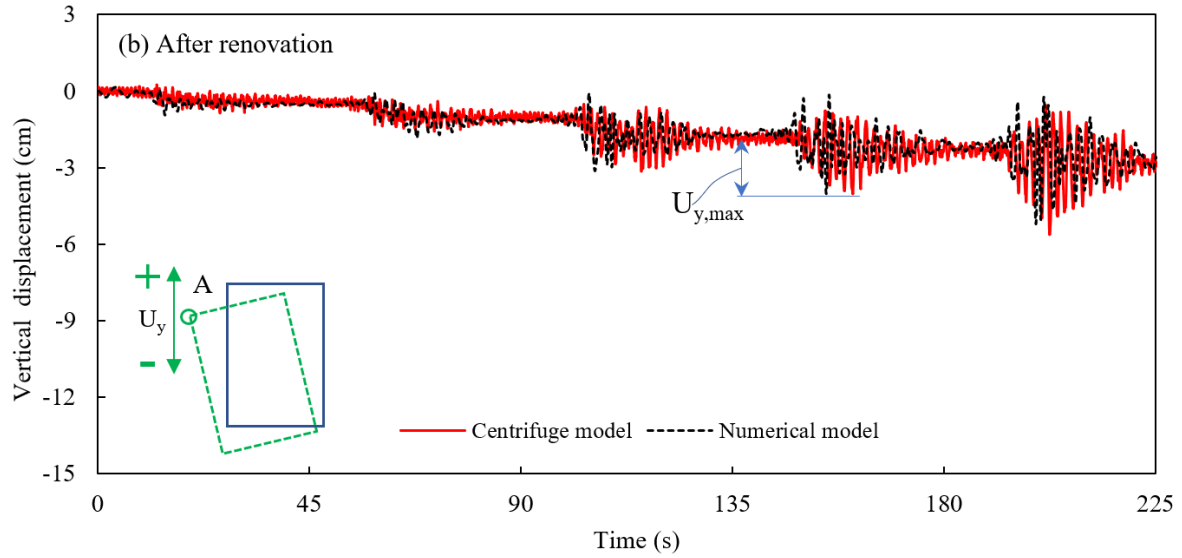

Maximum vertical displacement ($U_{y,max}$) at each step

(Unit: cm)	Step 1	Step 2	Step 3	Step 4	Step 5
Centrifuge model	-0.90	-1.31	-2.10	-2.03	-3.48
Numerical model	-0.94	-1.33	-1.97	-2.23	-3.25

Fig. 10 Vertical displacements at top left corner (Point A) of caisson

criteria value. After renovation, the maximum horizontal displacement reduced to 18.52 cm, and the ratio U_x/H decreased significantly to 1.05%. Therefore, it can be concluded that the renovation could decreased significantly damage that can be occurred in the main body of the quay wall under earthquake loading.

The comparison between the numerical analysis and centrifuge experiment results showed the same tendency for the horizontal and vertical directions, both before and after the renovation. It was generally observed that the displacements estimated from the FE models agreed well with the test results, although the predicted displacements were slightly lower than the measured values for almost all the steps. Both the centrifuge test and numerical analysis indicated that the horizontal displacement of the caisson after the renovation was reduced by approximately 10–25%, while the reduction for the vertical component was approximately 20–50%.

Fig. 11 compares the values for tilting of the caisson from the FE models and centrifuge tests for both cases. As can be seen from the graph, the results from the numerical analysis and centrifuge model coincided qualitatively. The

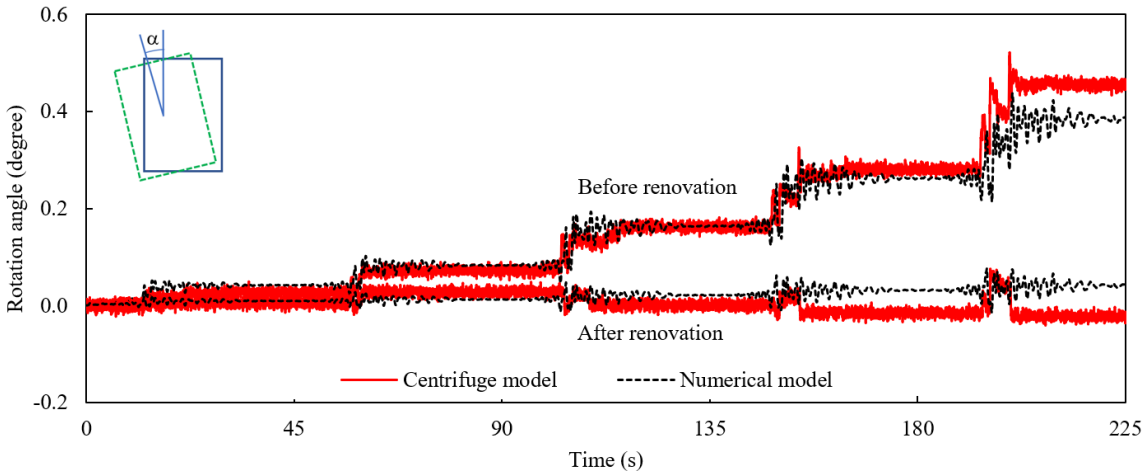

Fig. 11 Tilting of caisson for both cases

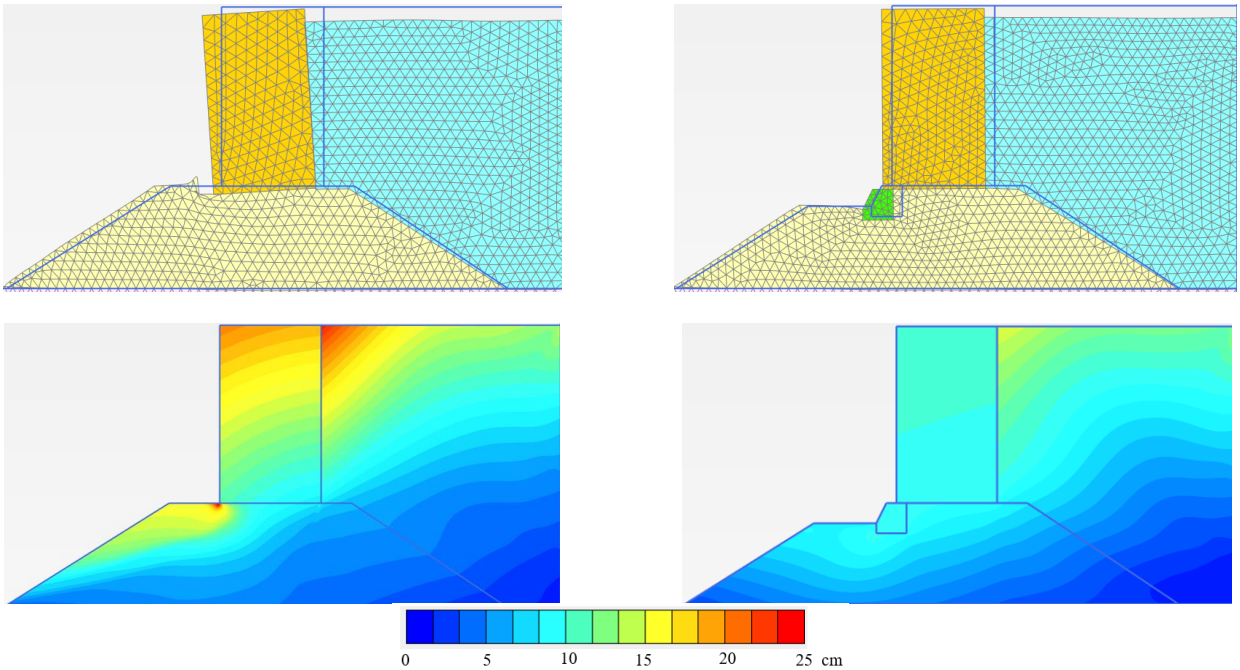

(a) Case 1- Before renovation (b) Case 2 - After renovation

Fig. 12 Deformation of quay walls at end of shaking

caisson in case 1 tilted toward the sea by approximately 0.5° at the end of the shaking, whereas in case 2, the caisson only slipped horizontally. This can be seen more clearly through the deformation around the quay wall at the end of the shaking, as plotted in Fig. 12. The upper part of the figure shows the deformed mesh (scaled up 10 times), while the lower part shows the displacement of the whole quay wall in the color scale. As shown in Fig. 12(a), in case 1, the rubble mound in front of the quay wall moved significantly. This indicated that the rubble in this area was locally unstable and tended to slip under earthquake loading. As a result, the settlement at the seaside was larger than that at the backfill side, and the caisson overturned toward the seaside. This trend also completely matched the result reported at the Rokko Island port after the Kobe earthquake of 1995 (Inagaki *et al*. 1996). In contrast, in case 2, the rubble area beneath the front toe of the caisson was strengthened by the grout material with higher strength. As shown in Fig. 12(b), the stability of the rubble mound was ensured, and the displacement was relatively low. Therefore, the rubble mound surface was balanced, and the caisson moved horizontally without rotation. This result agreed well with the finding of the shaking table test performed by Mizutani and Kikuchi (2013) on the caisson-type quay wall with the stabilized mound. It was also found that the movement of the wall was mainly due to the deformation of the rubble and not caused by slippage at the interface between the caisson and rubble. These phenomena were confirmed by FE analyses, experiments, and measurements in real cases, as shown in previous studies (Inagaki *et al*. 1996, Galavi *et al*. 2013).

4.2 Response acceleration

This section considers the response acceleration to assess the change in acceleration and agreement between

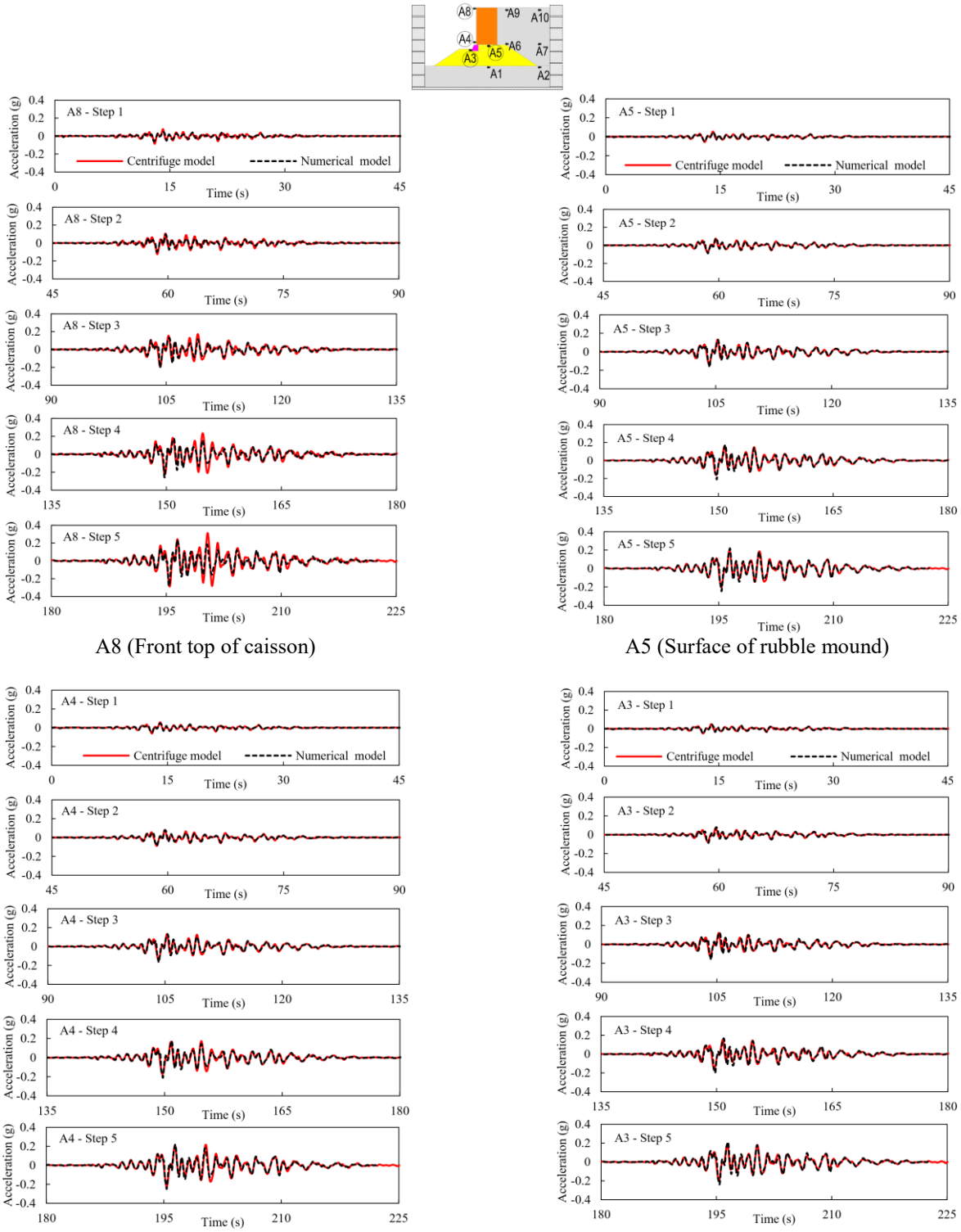

A8 (Front top of caisson) A5 (Surface of rubble mound)

A4 (Front toe of caisson) A3 (On the grouted rubble)

Fig. 13 Measured versus predicted acceleration time histories at location A3, A4, A5, A8

the numerical and experimental models. Figs. 13 and 14 plot the time history accelerations at some typical locations for case 2 (after renovation): A3 (on the grouted rubble), A5 (at the surface of the rubble), A4 (on the bottom left corner of the caisson), A8 (on the top left corner of the caisson), A6 and A9 (at the middle and top of the backfill, near the caisson, respectively), and A7 and A10 (at the middle and top of the backfill, near the boundary, respectively). It can be seen that the acceleration signal amplitudes increased significantly when the earthquake wave transferred from the base to the surface of the models. The comparison of the results between the centrifuge model tests and FE analyses demonstrated that the accelerations at the lower level (A3 to A7) showed good agreement. At the locations near the

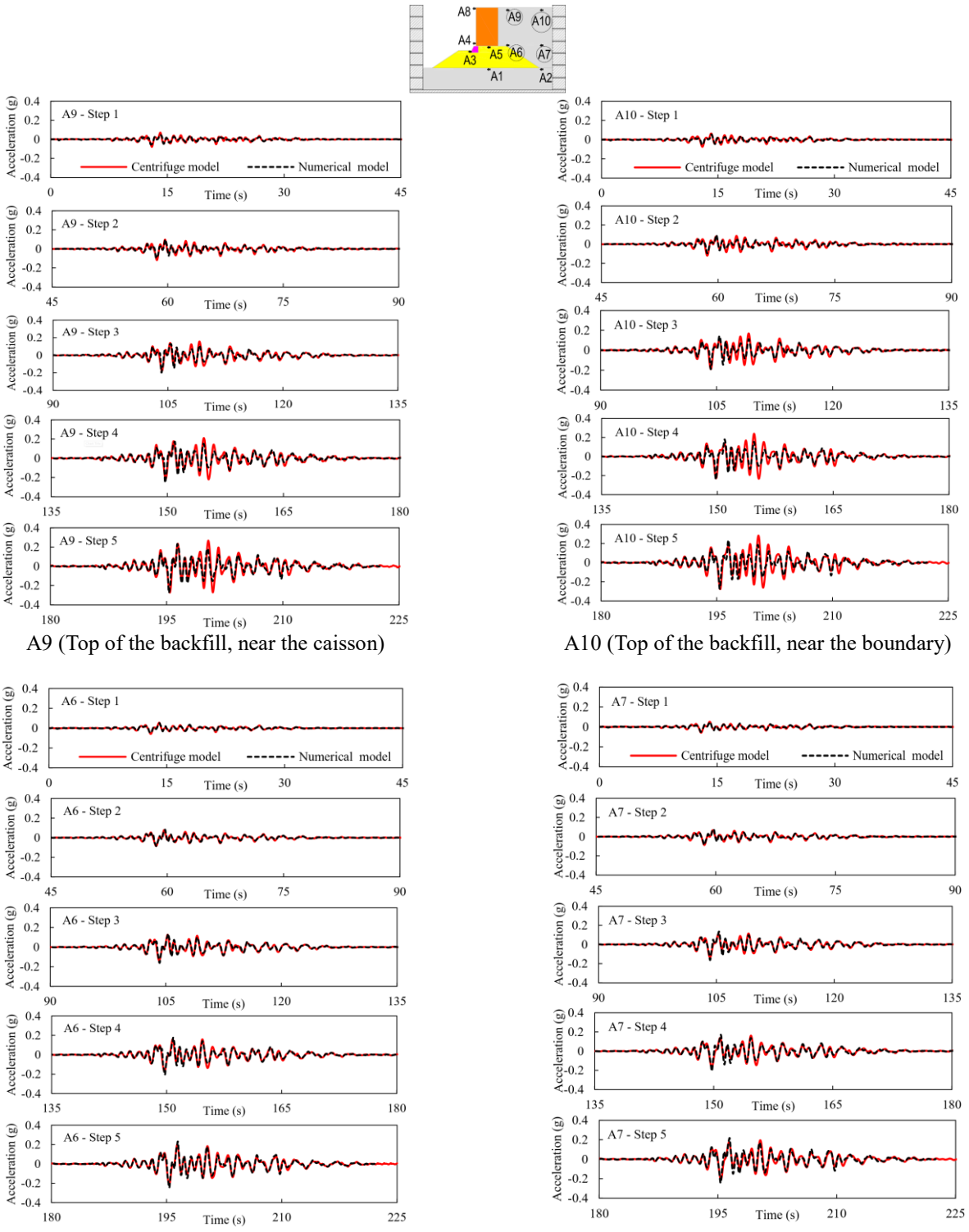

A9 (Top of the backfill, near the caisson) A10 (Top of the backfill, near the boundary)

A6 (Right shoulder of rubble mound) A7 (Middle of the backfill, near the boundary)

Fig. 14 Measured versus predicted acceleration time histories at locations A6, A7, A9, A10

surface (A8, A9, and A10), there was a moderate difference because some components of the experimental results had larger acceleration amplitudes.

To understand why the magnitude of the acceleration near the surface in the model test was larger than that of the numerical model at some points, the input and response waves were examined in detail in the frequency domain. Fig. 15 compares the Fourier spectra of the input motion at the base and output signals at location A8. There were some resonance points observed in the test results, especially at 0.83 s in step 1, 0.85 s in step 2, 1.04 s in step 3, and 1.23 s in steps 4 and 5. These occurred because the input motion contained signal components at these periods, and the oscillation amplitudes of the test model increased

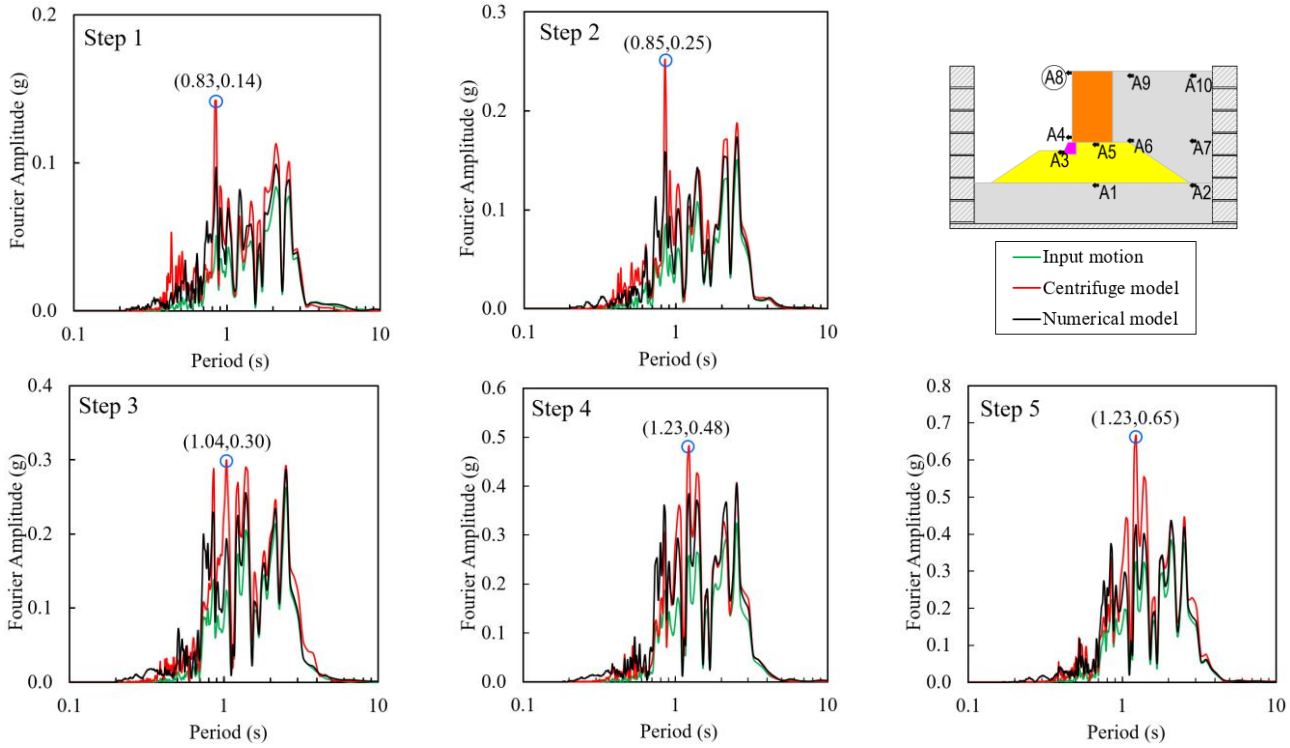

Fig. 15 Comparison of Fourier amplitudes among input motion, output of centrifuge model, and output of numerical model at point A8 (case 2)

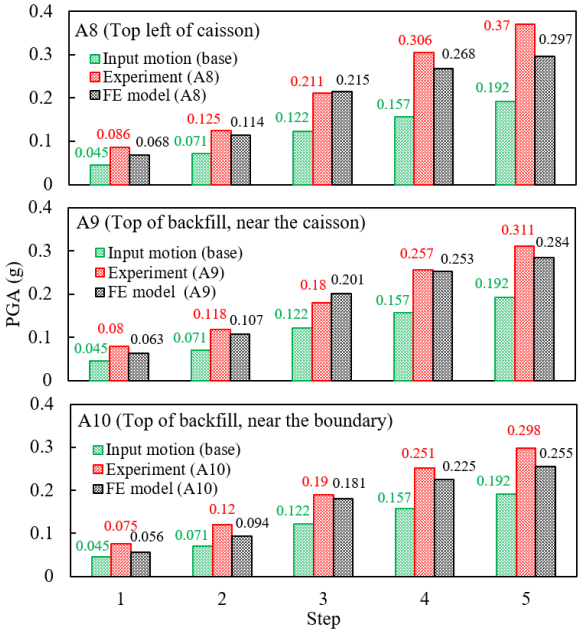

Fig. 16 PGA (g) values at A8, A9, and A10 (case 1)

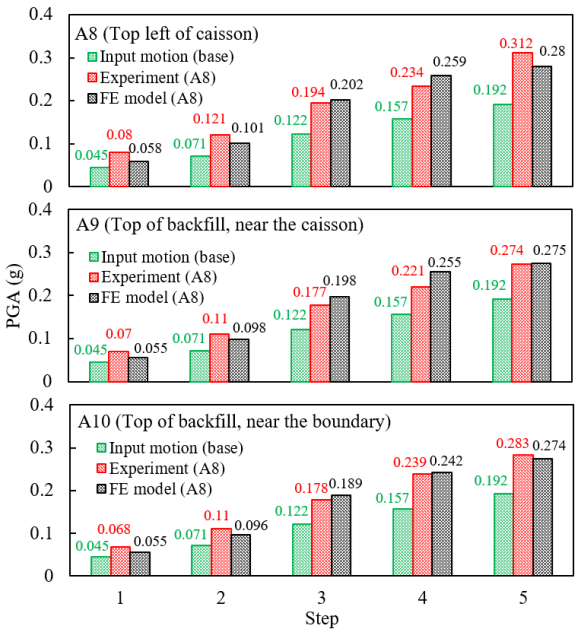

Fig. 17 PGA (g) values at A8, A9, and A10 (case 2)

dramatically. However, in the FE model, these resonance periods were not observed. This implied that the numerical simulation could not consider this phenomenon.

Fig. 16 presents the peak ground accelerations (PGAs) at A8, A9, and A10 near the surface of the models for case 1 (before renovation), while Fig. 17 shows the values for case 2 (after renovation). Table 5 summarizes the peak accelerations recorded in the centrifuge test at accelerometers A6 (near the base of the caisson) and A9 (near the surface of the caisson) for both cases. In the figures and table, the PGAs in the models was also compared to the PGA of the input wave at the base.

The comparison between the two cases showed that the PGA at the model surface of case 1 was larger than that of case 2. As shown in Figs. 16 and 17, in the 1st step, the PGAs recorded at locations A8, A9, and A10 of case 1 in the experiment were 0.086 g, 0.080 g, and 0.075 g, respectively, and from the numerical analysis, they were

Table 5 Measured PGAs (g) in backfill right behind caisson

	Case 1 - Before renovation					Case 2 - After renovation				
Step	1	2	3	4	5	1	2	3	4	5
A9	0.080	0.118	0.180	0.257	0.311	0.070	0.110	0.177	0.221	0.274
A6	0.052	0.080	0.134	0.171	0.217	0.059	0.085	0.137	0.171	0.218
a_{mean}	0.066	0.099	0.157	0.214	0.264	0.065	0.098	0.157	0.196	0.246
Input motion	0.045	0.071	0.122	0.157	0.192	0.045	0.071	0.122	0.157	0.192

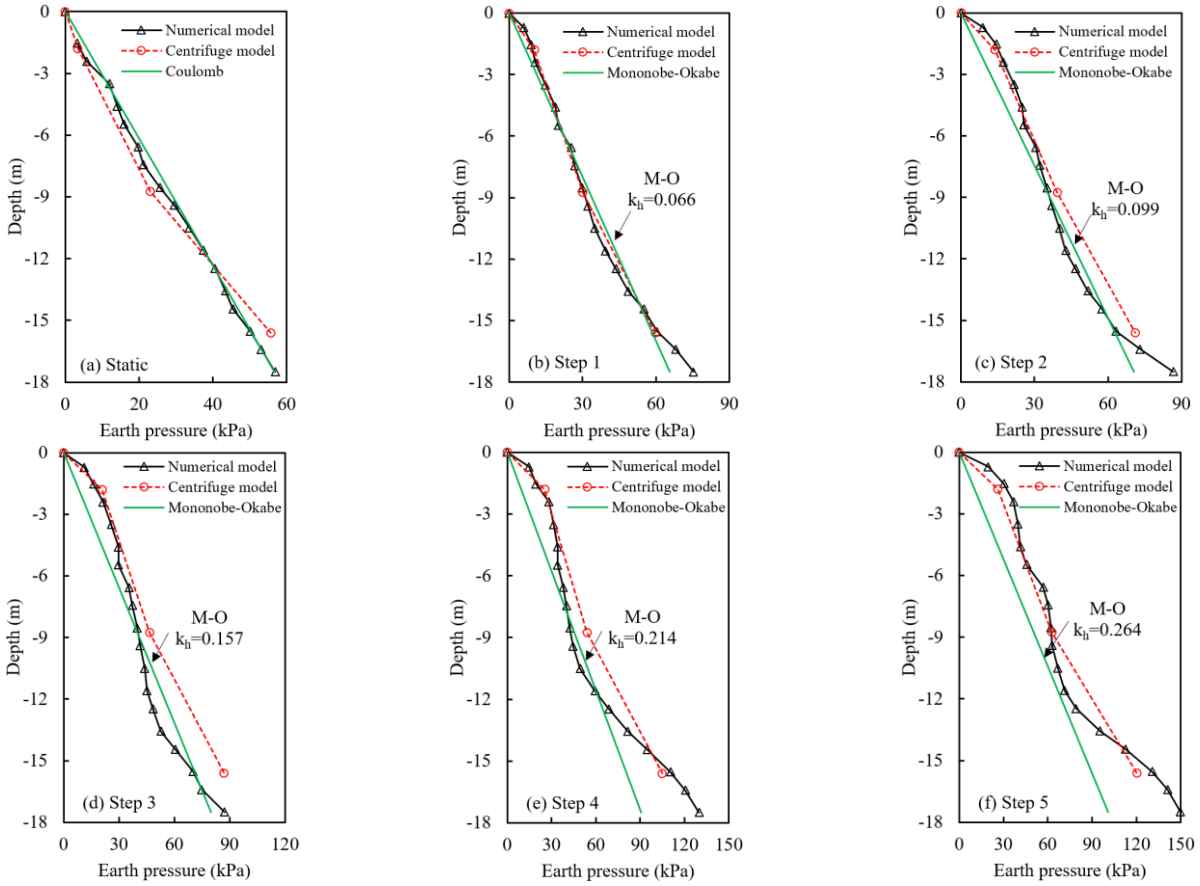

Fig. 18 Horizontal earth pressure acting on caisson before renovation

0.068 g, 0.063 g, and 0.056 g, respectively. In case 2, the measured PGAs were 0.080 g, 0.070 g, and 0.068 g, respectively, and the predicted PGAs were 0.058 g, 0.055 g, and 0.05 g, respectively. In the final step, the PGAs from the test at A8, A9, and A10 for case 1 were 0.370 g, 0.311 g, and 0.298 g, respectively, which were higher than those of case 2 at 0.312 g, 0.274 g, and 0.283 g, respectively. Similarly, the PGA values from the numerical analysis were 0.297 g, 0.284 g, and 0.255 g for case 1, respectively, and 0.280 g, 0.275 g, and 0.274 g for case 2, respectively.

In general, in both models the acceleration increased from the base to the surface. However, the acceleration in case 1 increased to a greater extent than that in case 2. In addition, the results observed in the backfill showed a lower magnitude compared to the PGA measured on the caisson. The results also indicated that the measured PGA was higher than the predicted values in almost all cases.

4.3 Earth pressure

Fig. 18(a) shows the distributions of the horizontal static earth pressure acting on the caisson before the renovation, while the dynamic earth pressures at a time when the maximum value occurred at each stage are plotted in Figs. 18 (b)-18(f). The earth pressures estimated by the FE model were compared with the resultlais measured by earth pressure gauges and calculated using analytical methods. In the analytical method, the earth pressures were calculated using Coulomb's theory for the static case and by the Mononobe–Okabe (M-O) theory for the dynamic case (Ministry of Ocean and Fisheries-Korea, 2018). The calculations were carried out using the soil with D_r = 70%. The mean acceleration (a_{mean}) at each step right behind the caisson was calculated in Table 5, and these results were used as horizontal seismic coefficients (k_h) to calculate the horizontal earth pressures using the M–O method.

As shown in Fig. 18(a), there was good agreement between the static earth pressure curves based on the FE method, analytical method, and experimental results. For the dynamic earth pressure, the results from the numerical analysis showed a trend similar to the measured curves,

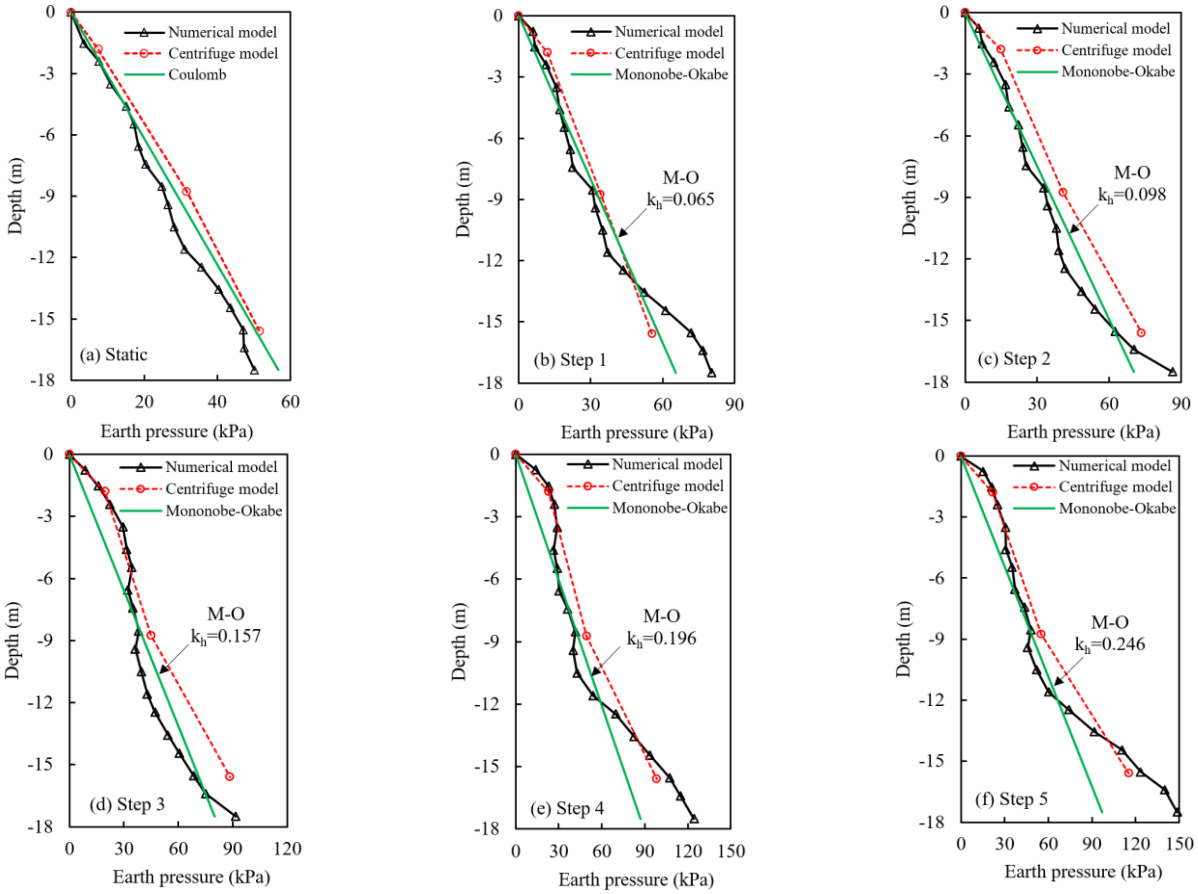

Fig. 19 Horizontal earth pressure acting on caisson after renovation

although the predicted value was slightly lower in some cases. Both the numerical and experimental results demonstrated that the horizontal earth pressure increased steadily with the depth and tended to increase sharply near the bottom of the caisson. This trend was also consistent with the results obtained from previous studies using centrifuge tests (Nakamura 2006) and numerical simulations (Dakoulas *et al*. 2018, Athanasopoulos-Zekkos *et al*. 2013, Rahaman and Raychowdhury 2017). A comparison with the calculations showed that the results of the FE model and centrifuge model were relatively compatible with the calculated results at the first two stages. From step 3 to step 5, the gap between the M–O lines and the other curves became larger. The experiments also showed higher values compared to the others. This difference occurred because all the M–O lines were calculated based on the soil parameters with relative density D_r = 70%, while the centrifuge tests and numerical analyses were conducted in five consecutive steps. After each step, because of the movement of the caisson, the properties of the sand immediately behind the caisson were changed, and the earth pressure was also different.

Similarly, a comparison of the horizontal earth pressures behind the caisson after the renovation is shown in Fig. 19. From Figs. 18 and 19, it can be observed that the difference in earth pressure between the two cases was relatively small at the respective steps. Thus, the two cases could be considered to have similar soil pressure distributions. This indicated that the grouting and deepening did not affect the earth pressure acting on the caisson. These results also agree well with the findings of the centrifuge test conducted by Khan *et al*. (2009) on existing sheet pile walls and sheet pile walls stabilized by seaside ground improvement.

5. Conclusions

The dynamic behaviors of a caisson-type gravity quay wall before and after renovation were evaluated and compared using centrifuge model tests and numerical analyses. The models were subjected to five consecutive input motions. The study considered the load–deformation behavior, seismic response, and earth pressure distribution. The conclusions of this study are as follows.

- The HS-small soil model was validated by comparison with the results of a RC test of silica sand. The results showed perfect compatibility between the experiment and numerical simulations in the description of how the shear modulus depended on the shear strain, and the relationship between the damping ratio and shear strain. This indicated that the HS-small model was suitable for describing the dynamic behavior of silica sand under the effect of an earthquake.
- The renovation of a quay wall not only increases its front water depth but also decreases the displacements of the caisson under earthquake loading. According to the results of this study, the horizontal displacement of the caisson after renovation was reduced by approximately 10–

25%, while the vertical displacement decreased by approximately 20–50%. The deformed shape of the quay wall under earthquake loading also changed after renovation. In the case of the existing quay wall, the caisson tended to tilt toward the seaside. After the renovation, the caisson exhibited a horizontal slip trend. This behavior was confirmed not only by the centrifuge tests but also by the FE models both qualitatively and quantitatively, although there were still some small differences. The results obtained in this study will be important reference data when designing upgrades for gravity quay walls.

- For both cases, the acceleration motions increased from the base to the surface of the model, and the acceleration on the caisson was larger than that of the backfill. However, the acceleration of the renovated quay wall increased more slowly than that of the existing quay wall. Thus, the PGA at the surface of the renovated quay wall model was lower than that of the existing case.
- The earth pressure distribution at the back of the caisson showed similar patterns before and after the quay wall renovation. This means that the rubble mound grouting and deepening did not change the earth pressure acting on the wall. The results also indicated that the dynamic earth pressure tended to increase to a greater extent near the bottom of the caisson.
- Centrifuge model tests were simulated by numerical models using the PLAXIS 2D V20 program. The numerical results, including the displacements of the caisson, deformed shapes of the quay walls, response accelerations, and earth pressures showed good agreement with the experimental results. This indicated that the numerical simulation proposed herein could describe the dynamic behavior of a caisson-type quay wall with relatively high precision. In addition, the renovation was technically feasible, and it could be considered to study further by testbed before applying in practice.

Acknowledgments

This research was a part of the project titled ‘Development of Design Technology for Safe Harbor from Disasters’ (No. 20180323), funded by the Ministry of Oceans and Fisheries, Korea.

References

Al-Homoud, A.S. and Whitman, R.V. (1995), “Comparison between fe prediction and results from dynamic centrifuge tests on tilting gravity walls”, *Soil Dynam. Earthq. Eng.*, **14**(4), 259-268. https://doi.org/10.1016/0267-7261(94)00051-H.

Alyami, M., Rouainia, M. and Wilkinson, S.M. (2009), “Numerical analysis of deformation behaviour of quay walls under earthquake loading”, *Soil Dynam. Earthq. Eng.,* **29**, 525-536. https://doi.org/10.1016/j.soildyn.2008.06.004.

Arablouei, A., Gharabaghi, A.R.M., Ghalandarzadeh, A., Abedi, K. and Ishibashi, I. (2011), “Effects of seawater-structure-soil interaction on seismic performance of caisson-type quay wall”, *Computers and Structures*, **89**, 2439-2459. https://doi.org/10.1016/j.compstruc.2011.06.005.

Athanasopoulos-Zekkos, A., Vlachakis, V.S. and Athanasopoulos, G.A. (2013), “Phasing issues in the seismic response of yielding, gravity-type earth retaining walls - Overview and results from a FEM study”, *Soil Dynam. Earthq. Eng.*, **55**, 59-70. https://doi.org/ 10.1016/j.soildyn.2013.08.004.

Bauduin, C., Mengeot, P. and Ganne, P. (2017). “Design and construction issues for deepening and strengthening of existing quay walls”, *Proceedings of the 19th International Conference on Soil Mechanics and Geotechnical Engineering*, Seoul, Korea.

Benz, T. (2007), “Small-strain stiffness of soils and its numerical consequences”, Ph.D. Dissertation, Universitat Sttutgart, Gemany.

Brinkgreve, R.B.J., Engin, E. and Engin, H.K. (2010). “Validation of Empirical Formulas to Derive Model Parameters for Sands.” *Proceedings of the 7th European Conference Numerical Methods in Geotechnical Engineering (NUMGE)*, Trondheim, Norway.

Cho, H.I., Kim, H.S., Sun, C.G. and Kim, D.S. (2020), “Settlement prediction for footings based on stress history from Vs measurements”, *Geomech. Eng.*, **20**(5) 371-384. http://dx.doi.org/10.12989/gae.2020.20.5.371.

Cho, H.I., Sun, C.G., Kim, J.H. and Kim, D.S. (2018), “OCR evaluation of cohesionless soil in centrifuge model using shear wave velocity”, *Geomech. Eng.*, **15**(4), 987-995. http://dx.doi.org/10.12989/gae.2018.15.4.987.

Chopra, A.K. (2001), *Dynamics of Structures: Theory and Applications to Earthquake Engineering*, 2nd Edition, Pearson Prentice Hall, Englewood, New Jersey, USA.

Cihan, H.K., Ergin, A., Cihan, K. and Guler, I. (2015), “Dynamic responses of two blocks under dynamic loading using experimental and numerical studies”, *Appl. Ocean Res.*, **49**, 72-82. https://doi.org/10.1016/j.apor.2014.11.003.

Dakoulas, P. and Gazetas, G. (2008), “Insight into seismic earth and water pressures against caisson quay walls” *Geotechnique*, **58**(2) 95-111. https://doi.org/ 10.1680/geot.2008.58.2.95.

Dakoulas, P., Vazouras, P., Kallioglou, P. and Gazetas, G. (2018), “Effective-stress seismic analysis of a gravity multi-block quay wall”, *Soil Dynam. Earthq. Eng.*, **115**, 378-393. https://doi.org/ 10.1016/j.soildyn.2018.08.032.

Galal, E.M. (2017), “A numerical study for upgrading the container terminal of port-said west port”, *Port-Said Eng. Res. J.*, **21**(2), 88-97. https://dx.doi.org/10.21608/pserj.2017.33296.

Galavi, V., Petalas, A. and Brinkgreve, R.B.J. (2013), “finite element modelling of seismic liquefaction in soils”, *Geotech. Eng.*, **44**(3), 55–64.

Gerolymos, N., Tasiopoulou, P. and Gazetas, G. (2015), “Seismic performance of block-type gravity quay-wall: numerical modeling versus centrifuge experiment” *Proceedings of the SECED 2015 conference on Earthquake Risk and Engineering towards a Resilient World*, Cambridge, UK.

Ha, I.S. and Han, J.T. (2016), “Evaluation of the allowable axial bearing capacity of a single pile subjected to machine vibration by numerical analysis”, *J. Geo-Eng.*, **22**(7). https://doi.org/10.1186/s40703-016-0036-5.

Ha, J.G., Lee, S.H., Kim, D.S. and Choo, Y.W. (2014), “Simulation of soil-foundation-structure interaction of Hualien large-scale seismic test using dynamic centrifuge test”, *Soil Dynam. Earthq. Eng.*, **61-62**, 176-187. https://doi.org/10.1016/j.soildyn.2014.01.008.

Iai, S., Tobita, T. and Nakahara, T. (2005), “Generalised scaling relations for dynamic centrifuge tests”, *Geotechnique*, **55**(5), 355-362. https://doi.org/10.1680/geot.2005.55.5.355.

Inagaki, H., Iai, S., Sugano, T., Yamazaki, H. and Inatomi, T. (1996), “Performance of caisson type quay walls at Kobe Port”, *Soils Foundations*, 119-136. https://doi.org/10.3208/sandf.36.special_119.

Khan, M.R.A., Hayano, K. and Kitazume, M. (2009), “Behavior

of sheet pile quay wall stabilized by sea-side ground improvement in dynamic centrifuge tests", *Soils Foundations*, **49**(2), 193-206. https://doi.org/ 10.3208/sandf.49.193.

Kim, D.S., Kim, N.R., Choo, Y.W. and Cho, G.C. (2013), "A newly developed state-of-the-art geotechnical centrifuge in Korea", *KSCE J. Civil Eng.*, **17**(1), 77-84. https://doi.org/10.1007/s12205-013-1350-5.

Kuhlemeyer, R.L. and Lysmer, J. (1973), "Finite element method accuracy for wave propagation problems", *Soil Dynam. Division*, **99**(SM5), 421-427. https://doi.org/10.1061/JSFEAQ.0001885.

Lee, C.J. (2005), "Centrifuge modeling of the behavior of caisson-type quay walls during earthquakes", *Soil Dynam. Earthq. Eng.*, **25**(2), 117-131. https://doi.org/ 10.1016/j.soildyn.2004.10.011.

Ministry of Ocean and Fisheries (2018), *Harbor and Fishing Port Design Standard*, Ministry of Ocean and Fisheries; Sejong, Republic of Korea.

Mizutani, T. and Kikuchi, Y. (2013), "Shaking table tests on caisson-type quay wall with stabilized mound", *Proceedings of the 18th International Conference on Soil Mechanics and Geotechnical Engineering: Challenges and Innovations in Geotechnics, ICSMGE 2013*, Paris, August.

Nakamura, S. (2006), "Reexamination of Mononobe-Okabe theory of gravity retaining walls using centrifuge model tests", *Soils Foundations*, **46**(2), 135-145. https://doi.org/10.3208/sandf.46.135.

Ngo, V.L., Kim, J.M. and Lee, C. (2019), "Influence of structure-soil-structure interaction on foundation behavior for two adjacent structures: Geo-centrifuge experiment", *Geomech. Eng.*, **19**(5), 407-420. http://dx.doi.org/10.12989/eri.2019.19.5.407.

Nguyen, A.D., Kim, Y.S., Kang, G.O. and Kim, H.J. (2021), "Numerical analysis of static behavior of caisson-type quay wall deepened by grouting rubble-mound", *J. Geo-Eng.*, **12**(1), 1-16. https://doi.org/ 10.1186/s40703-020-00130-3.

Obrzud, R.F. and Truty, A. (2018), *The Hardening Soil Model - A Practical Guidebook*, Zace Services Ltd., Preverenges, Switzerland.

Oung, O. and Brassinga, H. (2015), "Uncertainties in Redesigning an Existing Quay Wall." *Proceedings of the 5th International Symposium on Geotechnical Safety and Risk*, Rotterdam, October.

Pitilakis, K., Kirtas, E., Sextos, A., Bolton, M., Madabhushi, G. and Brennan, A. (2004), "Validation by Centrifuge Testing of Numerical Simulations for Soil-Foundation-Structure Systems." *Proceedings of the 13th World Conference on Earthquake Engineering*, Vancouver, August.

PLAXIS (2018), *Material Models Manual*, Bentley Systems, PA, USA.

Rahaman, O. and Raychowdhury, P. (2017), "Seismic active earth pressure on bilinear retaining walls using a modified pseudo-dynamic method", *J. Geo-Eng.*, **8**(1), 1-24. https://doi.org/10.1186/s40703-017-0040-4.

Ruggeri, P., Fruzzetti, V.M.E. and Scarpelli, G. (2019), "Renovation of Quay Walls to Meet More Demanding Requirements: Italian Experiences", *Coastal Eng.*, 1**47**, 25-33, https://doi.org/10.1016/j.coastaleng.2019.01.003.

Schanz, T., Vermeer, P. and Bonier, P. (1999). "Formulation and verification of the hardening soil model", *Beyond 2000 in Computational Geotechnics*, Routledge, London, United Kingdom.

Zeng, X. and Schofield, A.N. (1996), "Design and performance of an equivalent-shear-beam container for earthquake centrifuge modelling", *Geotechnique*, **46**(1), 83-102. https://doi.org/10.1680/geot.1996.46.1.83.